

# The crystallization mechanism of high-cordierite glass

KOICHI WATANABE

*Department of Chemistry, Faculty of Technology, Gunma University, Kiryu, Gunma 376, Japan*

EDWARD A. GIESS, MERRILL W. SHAFER

*IBM T. J. Watson Research Centre, Yorktown Heights, NY 10598, USA*

The crystallization mechanism of high-cordierite ( $2\text{MgO} \cdot 2\text{Al}_2\text{O}_3 \cdot 5\text{SiO}_2$ ) from a bulk-glass containing  $\text{B}_2\text{O}_3$  and  $\text{P}_2\text{O}_5$  as nucleating agents was studied using X-ray diffraction, differential thermal analysis and a polarizing microscope. Thin glass specimens, with a mirror surface, were heated rapidly in an electric furnace in the temperature range 888 to 1363° C for a desired time and then rapidly quenched to room temperature. The normal rate of growth of precipitated cordierite crystals was measured and their morphological change was observed photographically. The growth rate increased with temperature, and the maximum rate occurred at about 1250° C. The crystal morphology was hexagonal-prismatic, elongated along the *c*-axis. Faceted interface morphology was observed when the range of undercooling was from 7 to 174° C. Judging from the relationship between the reduced growth rate and the degree of undercooling, the crystallization mechanism in the range of lower undercooling was governed by a layer growth depending on the surface nucleation mechanism. In the range of higher undercooling, continuous growth was seen and at intermediate undercooling a transition range from a layer growth to a continuous growth was evident.

## 1. Introduction

High-cordierite ( $2\text{MgO} \cdot 2\text{Al}_2\text{O}_3 \cdot 5\text{SiO}_2$ ) glass-ceramic, belongs to the orthorhombic system and is pseudo-hexagonal-prism shaped elongated along the *c*-axis. It is a powerful and useful material for the fabrication of integrated circuit devices in the silicon semiconductor industry as it has a similar expansion to silicon, high deformation temperature, high chemical durability, high mechanical strength, and high volume resistivity. Therefore, many papers on the glass-ceramics of this system have already been published, especially concerning the effects of various nucleating agents (such as  $\text{TiO}_2$ ,  $\text{ZrO}_2$ ,  $\text{P}_2\text{O}_5$ , and alkali oxides) and the heat-treatment history of glass samples (such as nucleation and crystallization temperatures and holding times) upon their mechanical, thermal and electric properties [1–3]. Several papers on the crystallization

mechanism have also been reported, based on the data obtained using powdered glass samples, rather than bulk glass, as a starting material [4].

The rate of crystal growth from the melt may be controlled by any of four factors: (a) interface kinetics – the movement of material across the interface and its attachment to the crystal surface; (b) material transfer – the diffusion of material in the melt; (c) heat transfer – the removal of latent heat of crystallization from the growing crystal surface; (d) reconstructive transformation – the arrangement of atoms or ionic species at the solid-liquid interface [5]. In general, it is expected that for most glass bodies crystallizing at a small degree of undercooling the rate-controlling process will be the interface reaction of (a), as described above [6]. The growth mechanism of the crystal from the melt by the interface reaction can be classified

into two main types: continuous growth and layer growth. Continuous growth allows the interface to advance everywhere concurrently. Layer growth occurs by the movement of elementary steps across the crystal surface under conditions of small undercooling. This is commonly divided into two mechanisms: surface nucleation and spiral growth. The former is growth by two-dimensional nucleation taking place on the flat surface of the crystal. Surface nucleation growth, with a high degree of undercooling can become faster than spiral growth caused by screw dislocation.

The growth mechanism of a crystal can be anticipated by making *in-situ* observations of the surface of the growing crystal or by measuring precisely the relationship between the normal growth rate and the degree of undercooling. One can predict the mechanism by using an  $\alpha$ -factor proposed by Jackson [7] as a criterion for predicting the roughness of the solid-liquid interface. Jackson's  $\alpha$ -factor is represented by the following expression,  $\alpha = \xi \Delta H / T_M R$ , where  $\xi$  is the fraction of the total binding energy per molecule, in a plane parallel to the interface ( $\Delta H$  is the molar heat of fusion,  $T_M$  is the melting point and  $R$  is the gas constant). The value of  $\xi$  varies from 0 to 1, and is greater than 0.5 for the most closely packed crystallographic planes and less than 0.5 for less closely packed planes. For  $\alpha \leq 2$  the solid-liquid interface is predicted to be rough and for  $\alpha \geq 3$  it is smooth. If a solid-liquid interface is atomically rough, continuous growth with non-faceted interface morphology occurs and anisotropy of the growth rate is small; in addition, curved growth banding is generally expected. If the interface is atomically smooth, layer growth with faceted interface morphology occurs, either by a surface nucleation growth mechanism or by a screw dislocation mechanism. In this case, the growth rate is highly anisotropic and the crystal will be bound by crystallographic faces, and straight parallel growth banding will appear.

To elucidate the growth mechanism, Equation 1 using the reduced growth rate (viscosity  $\times$  growth rate) has been extensively used [8].

$$U_r = \frac{u\eta}{[1 - \exp(-\Delta H \Delta T / R T T_M)]} \quad (1)$$

Here,  $u$  is the normal growth rate,  $\Delta T$  is the undercooling and  $\eta$  is the viscosity. The  $U_r$  versus  $\Delta T$  relationship should give for continuous growth a horizontal line, for screw dislocation growth a

straight line of positive slope passing through the origin, and for surface nucleation growth a curve passing through the origin which exhibits positive curvature. For surface nucleation growth, a plot of  $\log U_r$  versus  $1/(T\Delta T)$  should give a straight line of negative slope.

The present paper is concerned with the crystal morphology and growth mechanism of high-cordierite precipitated from a bulk glass.

## 2. Experimental procedure

The glass used in the present study was prepared by melting together the required amount of each component in a platinum crucible at 1600°C for 2 h in an ambient atmosphere. Table I shows the glass composition, which was obtained by normal wet chemical analysis. For the crystallization studies, about 0.5 g of powdered glass was packed in a small platinum foil basket of 10 mm in diameter and 5 mm in depth, and remelted in an electric furnace at a temperature of 1500°C for 2 h. Thereafter, it was cooled rapidly to room temperature. An almost bubble-free glass plate about 2 mm in thickness was formed in the basket. The upper surface of the plate was polished on a 15  $\mu$ m diamond polishing plate to a thickness of 1 mm. Finally, the glass surface was polished to a mirror finish. Polished glass specimens were annealed for 5 h at 785°C, which is below the softening point of 805°C. Crystallization at a given temperature was performed by quickly heat-treating the glass for predetermined lengths of time, from 1 min to 30 h, and then rapidly quenching to room temperature. The crystallization temperature ranged from 888 to 1363°C. This corresponds to undercoolings from 482 to 7°C, respectively.

The furnace was controlled by a proportional controller (PID) with a Pt/Pt-10% Rh thermocouple, which maintained the desired temperature within  $\pm 2.0^\circ$  C. The temperature of the glass specimen was monitored by a digital thermometer placed in contact with the side of the platinum

TABLE I Glass composition

Component	wt %
SiO <sub>2</sub>	54.3
Al <sub>2</sub> O <sub>3</sub>	21.7
MgO	19.5
P <sub>2</sub> O <sub>5</sub>	1.7
Na <sub>2</sub> O	0.32
K <sub>2</sub> O	0.05
B <sub>2</sub> O <sub>3</sub>	1.0
Total	98.57

basket, the other was monitored discontinuously by a potentiometer with a calibrated thermocouple placed 0.5 mm away from the upper surface of glass specimen. In this paper the temperatures obtained by the potentiometer were used. The melting point, 1370°C, of high-cordierite used in this study was determined by observing the completely crystallized edge of a glass cube and from the differential thermal analysis (DTA) curve.

The growth length of the crystals was measured with a micrometer eye-piece at room temperature and their morphology was observed photographically. At temperatures greater than 1000°C, for short heating times, specimens were run singly. For long heating times (those in excess of 2 h) and at temperatures lower than 1000°C, they were run in groups of five or six. To measure the growth rates in the directions of the *c*- and *a*-axis, comparatively large crystals were chosen from among the many crystals precipitated. This was done because large crystals presumably nucleated during the early stages of nucleation. For each run, 20 measurements were made and averaged. After heat treatment, the back face of specimens was polished to a thickness of 0.5 mm by the method previously described. At each temperature, a plot of the length of the crystal versus time was constructed. The normal growth rate was obtained by taking one-half of the slope of the least-squares plot of the data.

Identification of the precipitated crystal phase was achieved using X-ray diffraction and a polarizing microscope. Viscosity in the temperature range 1100 to 1445°C was measured by a rotating cylinder method and in the range 705 to 1050°C by a parallel plate method. The rotating cylinder technique was calibrated with a standard viscous oil at a temperature of 20°C. The molar heat of fusion,  $\Delta H$ , of high-cordierite used in this study was 226 kJ mol<sup>-1</sup> (54 kcal mol<sup>-1</sup>) [9].

### 3. Results and discussion

Crystal growth was always observed to proceed from the glass surface toward the centre. There was no evidence of growth via homogeneous nucleation. Three crystal phases precipitated; high-quartz was observed only in the specimens treated in the temperature range 888 to 1248°C, protoenstatite in those treated in the range 1300 to 1363°C, and high-cordierite was observed over the entire temperature range. The normal growth rates of high-cordierite crystals were not seen to be influ-

enced by the coexistence of other phases. The morphological change of high-cordierite crystals as a function of the degree of undercooling is shown photographically in Figs 1a to d. Where the undercooling is from 7 to 70°C (see Fig. 1a) numerous high-cordierite crystals develop with a hexagonal-prismatic form bound by well-developed faces, together with long prismatic crystals of protoenstatite. It is clear that the layer growth mechanism is dominant in this temperature range. Crystals grown where the undercooling is from 70 to 174°C have a large hollow cone and have a hexagonal-prismatic or hexagonal-pyramidal form elongated along the *c*-axis (Fig. 1b). In addition, a large number of penetration twinned crystals and aggregative crystals were observed. Crystals growth in this range is also expected to be due to the layer growth mechanism. The numerous tiny crystals around the large crystal of high-cordierite are high-quartz. Figs 1c and d show two photomicrographs of representative crystals observed in specimens treated at undercoolings of 280 and 482°C. Crystals grown at an undercooling of 280°C have a fan type cellular structure on one side (Fig. 1c). This suggests the initial stage of a transition from a layer growth mechanism to one of continuous growth. In the specimen treated at the largest undercooling, i.e. 482°C, many crystals with an irregular form and a cellular type structure are observed. This implies that the solid-liquid interface has a non-faceted morphology. As can be seen in Figs 1a to d, high-cordierite crystals growing bulk glass have a faceted interface morphology over the range of undercooling from 7 to 174°C. This is in agreement with the prediction of Jackson [7] for materials with large entropies of fusion ( $\alpha \geq 3$ ), where a layer growth mechanism by either screw dislocation or surface nucleation is expected. At undercoolings greater than 174°C, the layer growth was not observed. Thus it appears that in an undercooling range of 174 to 435°C a transition region from faceted growth to non-faceted growth occurs, and at an undercooling greater than 435°C, non-faceted interface growth becomes dominant and continuous growth occurs.

The growth length at a given temperature is not necessarily a linear function of time for all the undercoolings measured. It is a function of the degree of undercooling. For instance, in the undercooling range 435 to 482°C, the relationship between the growth length and the treatment is a positive curve. In the range 70 to 435°C, it is linear

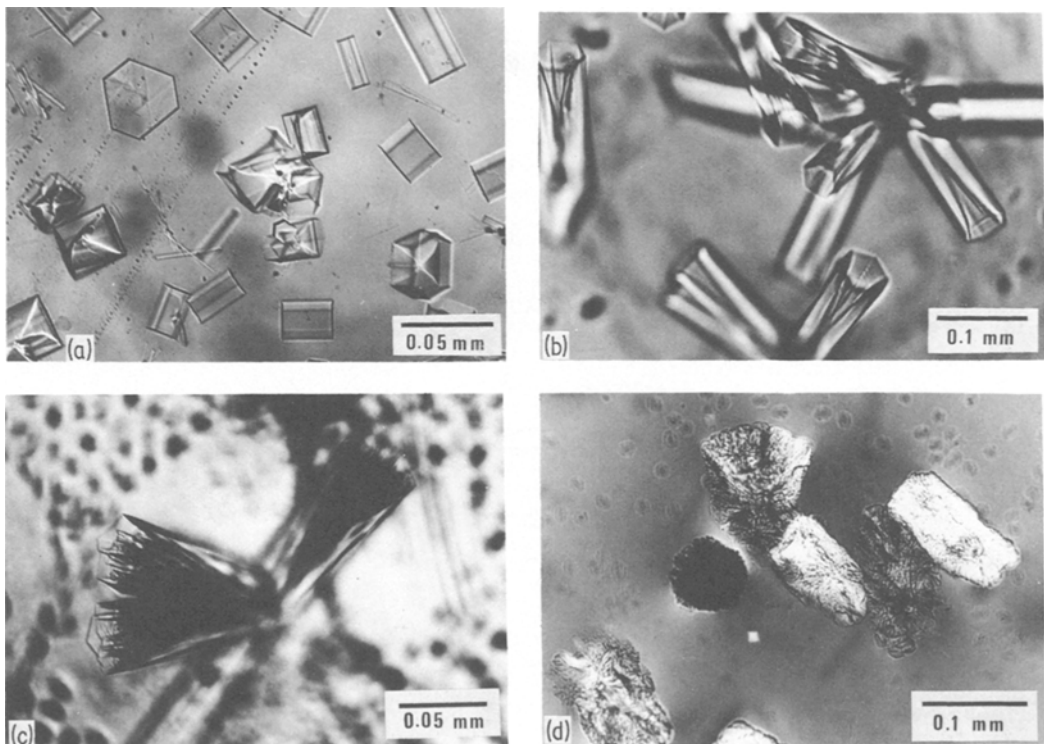


Figure 1 Morphological change of high-cordierite crystals depending on the undercooling  $\Delta T$ . (a)  $\Delta T = 7^\circ \text{C}$ . (b)  $\Delta T = 122^\circ \text{C}$ . (c)  $\Delta T = 280^\circ \text{C}$ . (d)  $\Delta T = 482^\circ \text{C}$ .

and for small undercooling (from 7 to  $70^\circ \text{C}$ ), it is negative. Figs 2a and b show some representative examples. We assume that the deviation from a linear relationship in the plots of the length versus time is due to a change of concentration gradient at the solid-liquid interface as a result of the

degree of undercooling. The normal growth rates along both the  $a$ - and  $c$ -axis at a given temperature were estimated from each plot in Figs 2a and b. In the case of negative or positive curves, they were estimated by taking one-half of the slope of the tangent for the respective curves passing through

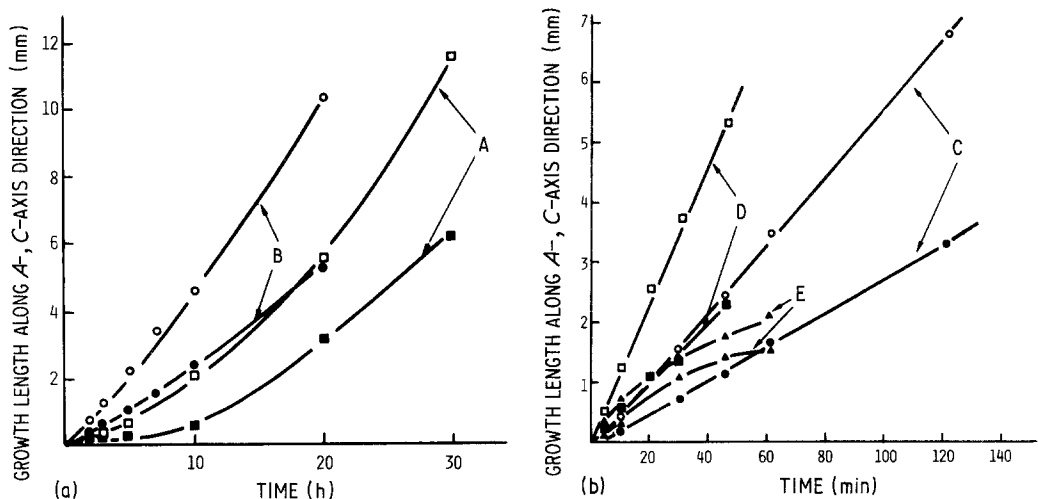


Figure 2 Growth length of crystals against heat-treatment time at different undercoolings. Open symbol:  $c$ -axis direction, closed symbol:  $a$ -axis direction. A  $\Delta T = 482^\circ \text{C}$ . B  $\Delta T = 459^\circ \text{C}$ . C  $\Delta T = 387^\circ \text{C}$ . D  $\Delta T = 334^\circ \text{C}$ . E  $\Delta T = 7^\circ \text{C}$ .

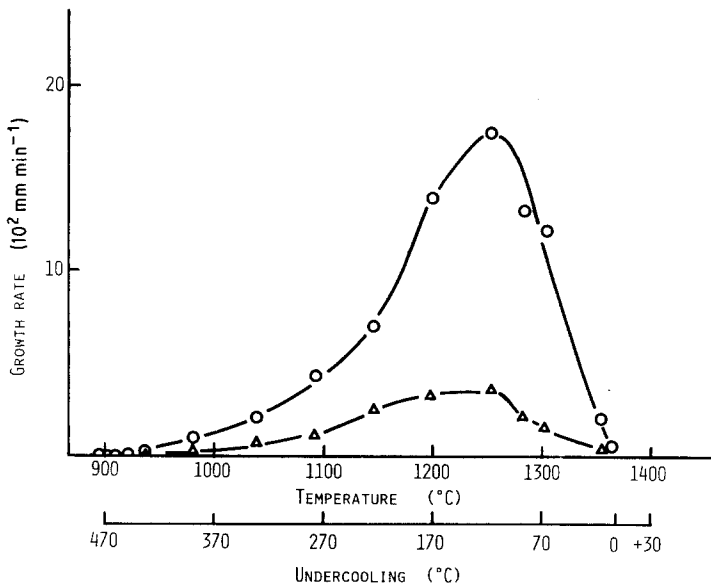


Figure 3 Relationship between the normal growth rates and the undercoolings.  $\circ$ : *c*-axis direction,  $\Delta$ : *a*-axis direction.

the origin [10]. In Fig. 3, the relationship between the normal growth rates and the undercooling (treatment temperature) is shown for both the *a*- and *c*-directions. In both directions, the maximum growth rate occurs at a temperature of about 1248°C. The growth rates extrapolate to zero at about 1367°C, which roughly corresponds to the melting point of high-cordierite crystals in the glass as determined by DTA, and also with the eutectic point of the cordierite and protoenstatite phases. On the low-temperature side, the zero-growth extrapolated temperature is about 885°C, which is a much higher temperature than that of the softening point of 805°C. The maximum growth rates in the respective directions are  $176 \times 10^{-3}$  (*c*-axis) and  $35 \times 10^{-3}$  (*a*-axis)  $\text{mm min}^{-1}$ , which are about 10 to 15 times larger than the normal growth rates of crystals growing from high-temperature solutions or aqueous solutions. The viscosity values of the present system are given in Table II. Using these viscosities and the growth rates in the respective direction, the reduced growth rates,  $U_r$ , were calculated from Equation 1 as a function of undercooling. The results obtained are summarized in Table II. The reduced growth rates increase exponentially with increasing undercooling. Fig. 4 shows an example in the *c*-axis direction. The steep positive slope suggests, as described before, that the growth of crystals in the present study may be taking place by a surface nucleation mechanism [6]. A plot of  $\log(u\eta)$  versus  $1/T\Delta T$  for both the *a* and *c* growth directions is shown in Fig. 5. It is seen that the relationship cannot be

described by a single line of negative slope, which would suggest a surface nucleation growth mechanism. Rather it displays appreciable curvature, which can be divided into two lines of negative slope, with the higher slope being observed at larger undercoolings and the lower slope, at smaller

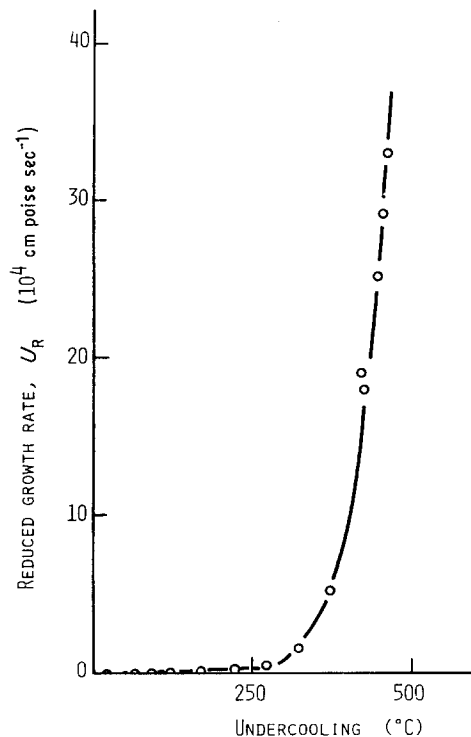


Figure 4 Plot of the reduced growth rate  $U_r$  in the *c*-axis direction as a function of the degree of undercooling.

TABLE II Normal growth rates and viscosity values at each crystallization temperature.

Temperature (° C)	$\Delta T$ (° C)	Growth rate, $u$ (mm min <sup>-1</sup> × 10 <sup>-3</sup> )		Viscosity, Log $\eta$ (Poise)	Reduced growth rate, $u/R$		Log ( $u\eta$ )		$1/T\Delta T$ (K × 10 <sup>-6</sup> )
		c-axis	a-axis		c-axis	a-axis	c-axis	a-axis	
1	888	0.44	0.15	8.87	3.3 × 10 <sup>5</sup>	1.2 × 10 <sup>5</sup>	5.52	5.06	1.141
2	900	0.91	0.46	8.49	2.9 × 10 <sup>5</sup>	1.5 × 10 <sup>5</sup>	5.46	5.16	1.147
3	911	1.35	0.68	8.28	2.5 × 10 <sup>5</sup>	1.3 × 10 <sup>5</sup>	5.41	5.11	1.154
4	927	2.67	1.37	7.84	1.8 × 10 <sup>5</sup>	0.9 × 10 <sup>5</sup>	5.25	4.97	1.164
5	935	3.60	1.86	7.73	1.9 × 10 <sup>5</sup>	1.0 × 10 <sup>5</sup>	5.28	4.99	1.169
6	983	10.16	4.99	6.72	5.3 × 10 <sup>4</sup>	2.6 × 10 <sup>4</sup>	4.73	4.41	1.206
7	1036	21.82	13.43	5.83	1.5 × 10 <sup>4</sup>	0.9 × 10 <sup>4</sup>	4.17	3.95	1.258
8	1090	44.32	15.36	4.79	2.8 × 10 <sup>3</sup>	1.0 × 10 <sup>3</sup>	3.45	3.98	1.327
9	1142	69.15	27.56	3.69	3.5 × 10 <sup>2</sup>	1.4 × 10 <sup>2</sup>	2.54	2.14	1.410
10	1196	140.35	32.97	2.89	1.2 × 10 <sup>2</sup>	2.8 × 10	2.04	1.41	1.523
11	1248	175.63	34.95	2.37	4.8 × 10	9.6	1.61	1.91	1.661
12	1280	133.12	18.97	2.07	2.1 × 10	2.9	1.19	9.35	1.738
13	1300	123.90	12.05	1.90	1.5 × 10	1.5	0.99	-0.02	1.834
14	1352	21.10	9.50	1.63	3.6	1.5	-0.05	-0.39	2.114
15	1363	5.16	4.75	1.59	1.5	1.3	-0.07	-0.74	2.183

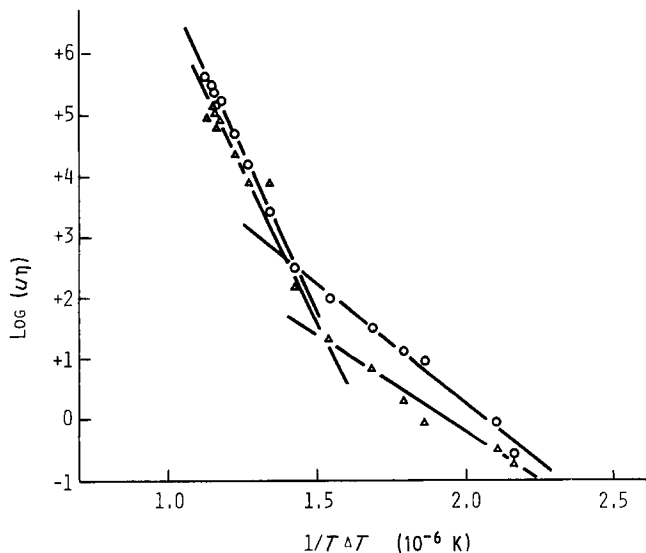


Figure 5 Relationship between  $\log(u\eta)$  versus  $1/T\Delta T$ . ○: *c*-axis direction, △: *a*-axis direction.

undercoolings. Similar behaviour has been observed in various systems [11]. This curvature has been attributed to a change in the surface energy with undercoolings [12]. Scherer and Uhlmann [13] obtained curved lines of negative slope, for the  $\log(u\eta)$  versus  $1/T\Delta T$  relationship, for organic compounds such as tri- $\alpha$ -naphthyl benzene, *o*-terphenyl, and  $\alpha$ -phenyl *o*-cresol, and calculated the values of the edge surface energy of nucleation with the undercooling from the higher and lower slopes. The surface energy calculated from the higher slope is in approximate agreement with that estimated by applying the surface nucleation model in the Turnbull–Staveley relationship. They showed, consequently, that in the region of larger undercoolings, the rate-controlling process is the surface nucleation growth mechanism. In the present study, however, in the region of smaller undercooling, i.e. 7 to 174°C, the growth mechanism of high-cordierite crystals is a layer growth mechanism with a faceted interface morphology; in the middle region of undercooling, i.e. 174 to 435°C, it is a transition range from layer growth to a continuous growth, and at larger undercooling, 435°C, cellular growth with a nonfaceted interface morphology becomes dominant. As can be seen in the photomicrographs of the morphological change of crystals displayed in Figs 1a to d, the growth mechanism of crystals in the present study is surface nucleation growth in the region of the lower slope at smaller undercoolings. This result is opposite to the result for the organic compounds by Scherer and Uhlmann [13], which indicated a faceted interface morphology over the full range of undercooling.

This discrepancy may be thought to be due to the differences in materials and experimental method and the thermodynamic properties of the respective systems.

#### 4. Conclusions

The crystallization mechanism of high-cordierite ( $2\text{MgO}\cdot 2\text{Al}_2\text{O}_3\cdot 5\text{SiO}_2$ ), containing a minor amount of  $\text{P}_2\text{O}_5$  as a nucleating agent, from a bulk glass was investigated by using XRD, DTA and a polarizing microscope.

1. All the crystals grew from the glass surface inward toward the centre. High-cordierite crystals can be observed over a large range of undercooling, i.e. 7 to 482°C. Two other phases, high-quartz and protoenstatite, precipitated only in a limited range of undercooling.

2. The external morphology of cordierite crystals changed from a hexagonal-prismatic form, bound by well-developed faces, to an irregular form having a cellular structure as the degree of undercooling increased. Faceted interface morphology, in the range of small undercooling, is in agreement with Jackson's theory, but not in the range of large undercoolings.

3. In the present study the maximum growth occurred at a temperature of about 1248°C, and the respective values in the directions of *c*- and *a*-axis are  $176 \times 10^{-3} \text{ mm min}^{-1}$  and  $35 \times 10^{-3} \text{ mm min}^{-1}$ .

4. A plot of  $\log U_r$  (normal growth rate  $\times$  viscosity) versus  $1/T\Delta T$  shows two lines of negative slope. The rate-controlling process in the range of small undercoolings, 7 to 174°C, can be described

as a layer growth mechanism via surface nucleation; in the middle range, 174 to 435° C, there is a transition region from a layer growth to a continuous growth mechanism, and at undercoolings greater than 435° C a continuous cellular growth mechanism, depending on a non-faceted interface morphology is dominant.

## References

1. A. G. GREGORY and T. J. VEASEY, *J. Mater. Sci.* **8** (1973) 333.
2. R. C. de VEKEY and A. J. MAJUMDAR, *Proc. Br. Ceram. Soc.* **25** (1975) 1.
3. R. MORRELL, *ibid.* **28** (1979) 53.
4. W. ZDANIEWSKI, *J. Amer. Ceram. Soc.* **61** (1978) 199.
5. V. J. FRATELLO, J. F. HAYS, F. SPAEPEN and D. TURNBULL, *J. Appl. Phys.* **51** (1980) 6160.
6. D. R. UHLMANN, in "Nucleation and Crystallization in Glasses", edited by J. H. Simmons, D. R. Uhlmann and Beall (American Ceramics Society, Columbus, Ohio, 1982).
7. K. A. JACKSON, in "Solidification", edited by T. J. Hughel and G. F. Bolling (American Society for Metals, Park, Ohio, 1970).
8. W. D. KINGERY, H. K. BOWEN and D. R. UHLMANN, "Introduction to Ceramics", (Wiley, New York, 1976).
9. A. NAVROTSKY and O. J. KLEPPA, *J. Amer. Ceram. Soc.* **56** (1973) 198.
10. F. C. FRANK, *Proc. R. Soc. A* **201** (1950) 586.
11. R. J. KIRKPATRICK, *Amer. Mineral.* **60** (1975) 798.
12. G. H. GILMER and P. BENNEMA, *J. Appl. Phys.* **43** (1972) 1347.
13. G. SCHERER and D. R. UHLMANN, *J. Crystal Growth* **15** (1972).

*Received 9 March  
and accepted 29 March 1984*